TMS target comparison identifies motor network reorganization associated with behavioral improvement in writer's cramp dystonia: A randomized, double-blind, Sham-controlled clinical trial

Author List: Noreen Bukhari-Parlakturk, MD, PhD*[1,2], Patrick J. Mulcahey[1], Michael W. Lutz, PhD[1], Rabia Ghazi, MD[1], Ziping Huang[1], Moritz Dannhauer, PhD[3], Pichet Termsarasab, MD[4], Burton Scott, MD PhD[1], Zeynep B. Simsek, MD[1], Skylar Groves[1], Mikaela Lipp[1], Michael Fei[1], Tiffany K. Tran[1], Eleanor Wood[5], Lysianne Beynel, PhD[6], Chris Petty[7], James T. Voyvodic, PhD[2,7], Lawrence G. Appelbaum, PhD[8], Hussein R. Al-Khalidi, PhD[9], Simon W. Davis, PhD[1,2], Andrew M. Michael, PhD[2], Angel V. Peterchev, PhD[2,10,11,12,13], Nicole Calakos, MD, PhD[1,2,14]

Affiliations:
[1]Department of Neurology, Duke University School of Medicine, [2]Duke Institute for Brain Sciences, Duke University, [3]Department of Computer Science, East Carolina University, Greenville, North Carolina,[4]Department of Medicine, Faculty of Medicine Ramathibodi Hospital, Mahidol University, Bangkok, Thailand, [5]Drexel University College of Medicine, Philadelphia, Pennsylvania, [6]Non Invasive Neuromodulation Unit, Experimental Therapeutics and Pathophysiology Branch, National Institute of Mental Health, National Institute of Health, Bethesda, Maryland, [7]Brain Imaging & Analysis Center, Duke University School of Medicine, [8]Department of Psychiatry, University of California, San Diego, California, [9]Department of Biostatistics and Bioinformatics, Duke University School of Medicine, [10]Department of Psychiatry and Behavioral Sciences, Duke University School of Medicine, [11]Department of Electrical and Computer Engineering, Duke University, [12]Department of Neurosurgery, Duke University School of Medicine, [13]Department of Biomedical Engineering, Duke University, [14]Department of Neurobiology, Duke University School of Medicine, Durham, North Carolina, USA.

ABSTRACT

Background: Writer's cramp (WC) dystonia is an involuntary movement disorder with distributed abnormalities in the brain's motor network. Prior studies established the potential for repetitive transcranial magnetic stimulation (rTMS) to either premotor cortex (PMC) or primary somatosensory cortex (PSC) to modify symptoms. However, clinical effects have been modest with limited understanding of the neural mechanisms hindering therapeutic advancement of this promising approach. **Objective:** This study aimed to understand the motor network effects of rTMS in WC that correspond with behavioral efficacy. We hypothesized that behavioral efficacy is associated with modulation of cortical and subcortical regions of the motor network. **Methods:** In a double-blind, cross-over design, twelve WC participants underwent weekly 10 Hz rTMS in one of three conditions (Sham-TMS, PSC-TMS, PMC-TMS) while engaged in a writing task to activate dystonic movements and measure writing fluency. Brain connectivity was evaluated using task-based fMRI after each TMS session. **Results:** 10 Hz rTMS to PSC, but not PMC, significantly improved writing dysfluency. PSC-TMS also significantly weakened cortico-basal ganglia, cortico-cerebellum, and intra-cerebellum functional connectivity (FC), and strengthened striatal connectivity relative to Sham. Increased PSC BOLD activity was associated with reduced dysfluent writing

behavior. **Conclusions:** 10 Hz rTMS to PSC improved writing dysfluency by redistributing motor network connectivity and strengthening somatosensory-parietal connectivity. A key signature for effective stimulation at PSC and improvement in writing dysfluency may be strengthening of intra-cortical connectivity between primary somatosensory and superior parietal cortices. These findings offer mechanistic hypotheses to advance the therapeutic application of TMS for dystonia.

***Corresponding author:**
Noreen Bukhari-Parlakturk,
DUMC Box 2900, Bryan Research Building
311 Research Drive
Durham, NC 27710
919-660-4104
noreen.bukhari@duke.edu

Word Count: 5,509

Key words: writer's cramp, motor network, transcranial magnetic stimulation, dystonia

Highlights:

- 10 Hz repetitive TMS to somatosensory cortex reduces writing dysfluency in dystonia
- Increased somatosensory cortex activity correlates with reduced writing dysfluency
- In untreated dystonia, writing dysfluency correlates with cerebellar connectivity.
- 10 Hz rTMS to somatosensory cortex induces reorganization of the motor network
- Somatosensory-parietal connectivity may be a key signature for effective TMS

Abbreviations:

PSC: primary somatosensory cortex, PMC: motor and premotor cortex, WC: writer's cramp dystonia

Running title: Motor network reorganization improves WC.

1. Introduction

Writer's cramp (WC) dystonia is an adult-onset focal dystonia (1). Patients develop involuntary co-contractions of hand and arm muscles during the specific task of writing, resulting in abnormal and often repetitive upper limb postures that can be painful and functionally disabling (2). There are no disease-modifying therapies for dystonia, and current treatments provide symptomatic benefit that is short-lived and variable.

Repetitive transcranial magnetic stimulation (rTMS) is a noninvasive brain stimulation technology that, in a meta-analysis of 27 prior studies, showed some benefit in reducing dystonia symptoms (3). Across these studies, a predictor of benefit was the stimulation site, which varied according to the dystonia subtype. In dystonias outside of the upper

limb, such as cervical dystonia and blepharospasm, some behavioral benefits were reported after TMS to the cerebellum (2/6) and anterior cingulate cortex (3/3), respectively. In upper limb dystonia, behavioral benefit was reported after TMS to motor-premotor cortex (PMC) (9/18 studies) or primary somatosensory cortex (PSC) (1/18 studies) (3-5). Although PSC only showed benefit in one study, it is noteworthy that the reported behavioral benefit was more enduring (two to three weeks) than any of the nine PMC studies (3-5). To best resolve whether one target site is superior, a head-to-head comparison of PMC versus PSC target controlling for the other variables among these studies would be necessary.

In addition to the stimulation site, another predictor of TMS benefit was the stimulation parameters. In upper limb dystonia, behavioral benefit was reported after 1 Hz rTMS (6/18 studies), 0.2 Hz rTMS (1/18 studies), and continuous theta burst (TBS) TMS (2/18 studies), while in cervical dystonia and blepharospasm, only TBS-TMS (2/5 studies) and 0.2 Hz rTMS (3/3 studies) showed benefits respectively (3). Overall, some behavioral benefits were reported after TMS in adult focal dystonias, but these varied according to dystonia subtypes, with key factors being stimulation site and stimulation parameters.

To improve the clinical efficacy of TMS in dystonia, more clinical studies are needed to directly compare the previously effective stimulation sites and parameters within subject. In addition, advances in our understanding of the brain mechanism mediating TMS benefit irrespective of brain disorder is critical to enable future rational optimization of this promising noninvasive therapeutic modality. In Parkinson's disease, for example, 10 Hz rTMS to the motor cortex was shown to increase dopamine release from the basal ganglia (4). In Wilson's disease, the same 10 Hz rTMS protocol to the motor cortex improved upper limb dystonia (5). Taken together, these independent studies suggest that 10 Hz rTMS to the motor cortex may improve upper limb dystonia by modifying subcortical regions of the motor circuit. No study to date has tested the role of 10 Hz rTMS in individuals with adult focal dystonias. Collectively, comparative and mechanistic TMS studies are critically needed to guide further refinements in TMS protocols to achieve clinically meaningful and enduring benefits across multiple dystonia subtypes.

Here, we aimed to build on prior TMS studies by directly comparing two stimulation sites that have reported efficacy in WC dystonia. We further aim to identify the brain mechanism mediating TMS-induced behavioral benefit by performing functional MRI in the acute stimulation period. The primary hypothesis was that the stimulation site that will show symptom benefit after TMS will modify key subcortical brain regions known to play a role in the dysfunctional motor network of dystonia. In a double-blind, cross-over study design, a 10 Hz rTMS was applied to either PMC or PSC and compared to Sham rTMS over the course of three independent sessions, allowing for a reliable within-subject comparison of stimulation site efficacy with several critical parameters being held constant.

2. Materials and methods:

2.1 Study design: The study was a double-blind Sham-controlled cross-over design with data collected at Duke University Hospital between September 2018 and September 2022. The study was approved by the Duke Health Institutional Review Board (IRB # 0094131), registered on clinicaltrials.gov (NCT 06422104), and performed in accordance with the Declaration of Helsinki. All participants gave written informed consent prior to any study participation. Inclusion criteria were adults (> 18 years), diagnosed with isolated right-hand dystonia by a Movement Disorder Specialist, more than three months from the last botulinum toxin injection, more than one month from trihexyphenidyl medication, and able to sign an informed consent form. Exclusion criteria were any contraindications to receiving MRI or TMS.

2.2 MRI data acquisition and preprocessing: All study participants completed a brain imaging scan pre-TMS, and those who qualified also completed it after each TMS visit. All anatomical and functional imaging data was collected on a 3 Tesla GE scanner equipped with an 8-channel head coil. The anatomical MRI scan was acquired using a T1-weighted echo-planar sequence with the following parameters: voxel size: 256 x 256 matrix, repetition time (TR) = 7.316 ms, echo time (TE) = 3.036 ms, field of view (FOV) = 25.6 mm, 1 mm slice thickness. During fMRI sequences, participants copied holo-alphabetic sentences on an MRI-compatible writing tablet. The sentence writing was performed in a block design alternated by rest blocks (**Fig. 1, task-fMRI panels**). The CIGAL software presented visual writing instructions and recorded participants' movements during the fMRI scan (6). *Pre-TMS fMRI*: Functional echo-planar images were acquired using the following parameters: voxel size: 3.5 x 3.5 x 4.0mm^3, flip angle 90°, TR = 2 s, TE = 30 ms, FOV = 22 mm for 37 interleaved slices in ascending order, writing block: 20 s, rest block: 16 s, total: 12 blocks per fMRI. *Post-TMS fMRI:* Functional echo-planar images were acquired with the following parameters: voxel size: 2.0 x 2.0 x 3.0mm^3, flip angle 90°, TR = 2.826 s, TE = 25 ms, FOV = 25.6 mm for 46 slices. Writing block: 20 s, rest block: 20 s, total: 5 blocks x 6 runs = 30 blocks per fMRI. fMRI images were preprocessed using fMRIPrep (7), as detailed in the supplementary methods. FMRIs with excessive head movements (defined as mean frame-wise displacement > 0.5 mm) were excluded from the study.

2.3 MRI signal analysis: Pre-processed pre-TMS fMRIs from were input into FEAT analysis in FSL software version 6.0 (FMRIB, Oxford, UK) to generate a subject-level statistical map. A general linear model in which writing task timing (block design) was convolved with a double-gamma hemodynamic response function to generate the statistical brain map. To account for head motions, fMRIprep reported regressors (CSF, white matter, framewise displacement, and motion outliers) were regressed out from each statistical map. Spatial smoothing with a Gaussian kernel of full-width half-maximum of 5 mm and temporal high pass filter cutoff of 100 seconds was applied during the FEAT analysis. A WC group-level statistical map was then computed by importing all WC participants' statistical brain maps from their baseline task-fMRI into a mixed-effects FLAME1 model.

2.4 Personalized TMS target selection: For each TMS study participant, a two-voxel cortical brain mask was generated for TMS targeting to the premotor and motor cortex (PMC) and for TMS targeting to the primary somatosensory cortex (PSC). To constrain

the stimulation target to the PMC and PSC regions, each participant's statistical brain map was overlayed on the WC group statistical brain map, and anatomical masks for precentral (for PMC) and postcentral gyrus (for PSC) from the Harvard-Oxford MNI atlas and the participant's anatomical scan. Two consecutive voxels in the anatomic region of the left precentral/postcentral gyrus, with peak activation in the participant's statistical map and the WC group statistical map and within 1 cm from the scalp surface were selected as the fMRI-guided PMC and PSC target for TMS delivery (**Fig. 1, target selection panel**). The fMRI-guided cortical brain masks were then used to perform prospective electric field (E-field) modeling on each participant's scalp, as detailed in the supplementary methods. The purpose of the modeling was to identify the optimal position and orientation of the TMS coil on the participant's scalp. This optimal coil setup was then used for the TMS intervention in the neuronavigation system (Brainsight, Rogue Research, Canada, version 2.4.9). The final personalized TMS targets at left PMC and left PSC for the 12 WC participants are shown overlayed on the MNI brain (**Fig. 2**).

2.5 TMS stimulation: Eligible participants received three TMS visits. The three TMS visits consisted of 10 Hz rTMS to PSC, 10 Hz rTMS to PMC, and Sham rTMS to PMC (**Fig. 1, rTMS panel**). Each rTMS visit was separated by a minimum of one week to allow signal washout. To negate any order effect, each participant was randomized to one of six possible orders for the three TMS conditions. All TMS was performed using an A/P Cool B65 coil attached to a MagVenture R30 device (MagVenture, Farum, Denmark). During each TMS visit, participants first completed an optimal motor cortex localization and motor threshold calculation as detailed in the supplementary methods (8). The active TMS paradigm delivered to each cortical target was 25 trains applied at 10 Hz rTMS with biphasic pulses and an inter-train interval of 10 seconds at 90% resting motor threshold (RMT) for a total of 1000 pulses delivered in a single block (~five minutes), while participants were sitting in a recliner. To ensure a consistent brain state and specifically target the stimulation to the motor network, each stimulation block was preceded by a writing block (~five minutes) in which participants performed a sentence copying task. A total of four blocks of TMS alternated with four writing blocks were performed (a total of 4000 pulses per TMS visit) (**Fig. 1, rTMS panel**). To perform Sham stimulation, the same AP coil was used in placebo mode, which produced clicking sounds and somatosensory sensation from scalp electrodes similar to the active mode but without a significant electric field induced in the brain (9). As previously reported, this type of stimulation allows participants to stay blinded during the experiment.

2.6 Retrospective TMS coil deviations: During each TMS block, data on the experimental TMS coil location and orientation was recorded every 500 ms in the neuronavigation system and snapped to scalp reconstruction mode prior to exporting it. Data was then imported into SimNIBS software (version 2.0.1 / 3.2.6) to calculate the deviations from the intended TMS coil position and orientation using the retrospective Targeting and Analysis Pipeline (TAP) (10). The TMS coil placement (position and orientation) data were first extruded outwards along the scalp normal by adjusting it for the participant's recorded hair thickness for each TMS visit. These TMS coil placement data were then used to compute the coil placement deviation from the optimized coil setup constructed during the prospective E-field modeling reported in the

supplementary methods. The deviations in the TMS coil placement were calculated in the normal and tangential planes and reported as changes in distance (mm) and angle (degrees). The direct distance between the actual and optimized target was also calculated, as previously reported (10, 11). Due to technical issues with the neuronavigation software, the experimental TMS coil location and orientation during one TMS block was excluded from one participant's Sham TMS visit.

2.7 TMS-induced behavior changes: During each TMS visit, participants performed a behavioral writing assay before and after each four-block TMS session (**Fig. 1, behavior assessment panels**). The behavioral assay consisted of participants using a sensor-based pen on a digital tablet (MobileStudio Pro13; Wacom Co, Ltd, Kazo, Japan). Participants copied a holo-alphabetic sentence ten times in a writing software (MovAlyzer, Tempe, AZ, USA). The sensor-based pen recorded the x, y, and z positions and the time function of the participants' writings. The writing software then automatically transformed the writing samples' position parameters and time functions using a Fast Fourier transform algorithm to calculate the kinematic features. A previously detailed analysis of these kinematic writing measures showed that the sum of acceleration peaks in a single sentence (henceforth peak accelerations) (**Fig. 1, behavior assessment panel, black circles**) demonstrates high diagnostic potential (sensitivity, specificity, and intra-participant reliability), and associates with patient-reported dystonia and disability scales (12). In this study, the peak accelerations measure was used as the primary behavioral outcome measure. Participants performed the behavioral assessment before and after each TMS session. To minimize learning across the three TMS visits, a different holo-alphabetic sentence was used for each sequential visit. The three sentences were: Pack my box with five dozen liquor jugs; The quick brown fox jumps over the lazy dog; Jinxed wizards pluck blue ivy from the big quilt. To measure the change in peak accelerations, each participant's post-TMS measure was normalized by the mean of their pre-TMS measure using the following equation: [(Post-TMS peak accelerations per sentence)/(mean peak accelerations for all ten sentences pre-TMS)]*100. Higher measures of peak accelerations represent greater writing dysfluency and worsening dystonia. The standard TMS adverse events survey and secondary outcome measures of clinician-rated and participant-reported dystonia scales were also collected before and after each TMS session as detailed in the supplementary methods.

2.8 TMS-induced fMRI changes: After each TMS visit, participants completed a task-based fMRI. The fMRI task design, acquisition settings, preprocessing, and run-level analyses are detailed in methods section 2.2 and 2.3 above. To compare changes in BOLD activity across the three TMS conditions, 4D time-series data were extracted from each fMRI run level FEAT directory using brain masks for regions of interest. The time-series data for each region of interest was z-scored across runs and analyzed as on-block and off-block writing epochs. To perform functional connectivity analysis, the extracted 4D time-series data for each region of interest was correlated pairwise using Pearson's correlation (R) and Fisher z-transformed.

2.9 Brain parcellation and ROI extraction: To compare BOLD activity and functional connectivity analysis across TMS conditions, brain masks corresponding to regions of

the motor network previously identified as abnormal in human dystonia studies were prepared (13-21). Anatomical brain masks were prepared using the Harvard-Oxford MNI brain atlas for the following subcortical regions: left caudate (CAU), left putamen (PUT), left globus pallidus (PAL), left thalamus (THL), left subthalamic nucleus (STN) and left substantia nigra (SN). Since the cortex and cerebellum are large brain regions, brain masks for these regions were made using the publicly available Dictionaries of Functional Modes (DiFuMo) brain atlas (22). DiFuMo is a fine-grain atlas that parcellated the brain into functional regions of 1024 components based on data from 15,000 statistical brain maps spanning 27 studies (22). To select DiFuMo brain masks for the left superior parietal cortex (SPC), left inferior parietal cortex (IPC), left supplementary motor area (SMA), and right cerebellar lobules VI and VIII (CBL), MNI coordinates from prior neuroimaging studies in dystonia were used (15, 23). For PSC and PMC, each participant's personalized TMS target (section 2.4) was used as the center to prepare a custom 5 mm spherical mask.

2.9 Statistical Analyses: Because the study was a cross-over design with multiple visits and measures, a Mixed Model for Repeated Measures (MMRM) statistical analysis was used to compare differences within participants across the three TMS conditions. For the measure of TMS coil deviations, the MMRM covariate was the TMS condition. For examiner rating scales, the covariates were TMS condition, TMS visit, and clinician rater. For patient rating scales, the covariates were TMS condition and TMS visit. For the measures of peak accelerations, BOLD activity, and functional connectivity analyses, the covariates were TMS condition, visit, and interaction of TMS condition*visit. Differences across participants were accounted for by including participants as a random effect variable. To focus on clinically meaningful differences induced by TMS, functional connectivities that showed small effect sizes (defined as Cohen's $D \leq |0.2|$) between active and Sham conditions were excluded from statistical analyses. Changes in BOLD activity during the on-block and off-block writing were analyzed separately using MMRM. To perform brain-behavior correlation, BOLD activity or functional connectivity was correlated within participants with their measure of normalized peak acceleration behavior using Pearson's (R). To compare differences in brain-behavior correlation across TMS conditions, a generalized regression analysis was performed. For the generalized regression, the dependent variable was peak accelerations, covariates were TMS conditions, BOLD activity or functional connectivity, and the interaction term (TMS condition*BOLD activity/functional connectivity). All MMRM were fit using restricted maximum likelihood. Covariance structures of the unstructured, autoregressive first order, and compound symmetry were tested and evaluated for stability of the model fit and ability to converge. Compound symmetry reached convergence for all of the models and, therefore, was utilized. All p values were corrected for multiple comparisons using the method of Benjamini-Hochberg, with an alpha of 0.05 accepted as statistically significant. For the exploratory functional connectivity to behavior correlational analysis, a less stringent alpha threshold of 0.1 was accepted as statistically significant.

RESULTS:

Clinical characteristics: Thirty-four participants were assessed for study eligibility (**Fig. 3**). Of those assessed for eligibility, 24 WC participants met the inclusion/exclusion criteria to participate in the TMS study and completed a baseline fMRI before the first stimulation visit. The baseline fMRI from five participants was excluded due to other neurological disorders, structural abnormalities on the MRI brain, or excess head motion. FMRIs from 19 WC participants were then used to identify a group-targeting approach for TMS. Of these 19 participants, 14 consented to participate in the TMS research visits. Two participants who consented to TMS visits were taking a medication that increased the risk of seizures and, therefore, were excluded from undergoing TMS. Twelve WC participants (11/1 males/female; mean age 55 [SD 12.91] years) completed all three TMS visits. Due to technical issues during data collection, one participant's TMS visit (Sham) was removed from the data analysis. Thus, data from 12 WC participants and 35 TMS visits (12 participants x 3 conditions – 1 visit = 35) were used for all analyses in this study. None of the 12 WC participants reported any adverse side effects of TMS. The mean symptom duration for the 12 WC participants was 16.4 years [SD 15.54].

No differences in TMS technical delivery: To evaluate the technical delivery of TMS, the position and orientation of the TMS coil during the three conditions were analyzed retrospectively. There were no significant differences in the position or orientation of the TMS coil across the three conditions (**Fig. 4 and Supplementary Table 1**). Therefore, TMS delivery across the three conditions was technically comparable.

10 Hz rTMS to PSC, but not PMC, improved writing dysfluency: In a within-participant comparative design, in which all participants received stimulation to both sites and at the same frequency, we found that 10 Hz rTMS to PSC significantly decreased writing dysfluency compared to Sham-TMS (**Fig. 5**) [PSC vs. Sham: -1.73, SE: 0.41, t(21): -4.22, p = 0.001] and PMC-TMS [PSC vs. PMC: -1.28, SE 0.40, t(21): 3.23, p = 0.012]. TMS to PMC did not show significant differences in writing dysfluency compared to Sham [PMC vs. Sham: -0.45, SE 0.41, t(21): -1.09, p = 0.639]. These results confirm prior studies that TMS can modify behavior in WC dystonia and show the first results using 10 Hz frequency, within-participant site comparisons, and delivery under a task-activated brain state. Across the clinician rating (BFM right arm dystonia and WCRS movement score) and participant-reported scales (BFM writing score and ADDS), there were small but consistent improvements in dystonia symptoms after PSC-TMS compared to Sham (**Supplementary Table 2**, “Difference” column, positive values represent an improvement, and negative values represent worsening dystonia). However, the effect sizes of these coarse categorical rating scales were small and had large variability, resulting in no statistical differences across the three TMS conditions.

10 Hz rTMS to both PMC and PSC decreased subcortical activity in the motor network. Considering the differential effect of the stimulation site on behavioral outcomes, we examined the extent to which TMS at these two target sites affected brain BOLD activity (**Fig. 6A**). Across the motor network, stimulation at each of the two TMS target sites showed similar patterns of brain activation (**Fig. 6B**). Specifically, 10 Hz rTMS decreased subcortical brain activity and increased BOLD activity at the superior parietal cortex. In the cerebellum, the brain activation pattern varied by TMS target site.

PMC-TMS decreased BOLD activity in lobules VI and VIII, while PSC-TMS decreased BOLD activity in lobule VI only. Overall, these results suggest that cortically delivered 10 Hz rTMS decreased deep brain activity in the motor network with an overall activation pattern that was similar across the two stimulation sites. Changes in BOLD activity after TMS, therefore, do not explain the differential effect of stimulation site on behavioral outcomes.

PSC-TMS modified subcortical connectivity, distinct from PMC-TMS. We next considered if the behavioral outcome differences between the stimulation sites also corresponded to changes in functional connectivity (FC) after TMS. **Figure 7** illustrates the changes in the magnitude of brain connections induced by PSC-TMS compared to Sham. In general, PSC-TMS weakened cortico-striatal connectivity (thin lines: PMC-CAU, PSC-CAU), cortico-cerebellar connectivity (SPC-CBLVI), and intra-cerebellar connectivity (CBL VI-VIII). PSC-TMS also strengthened striato-cerebellar connectivity (thick lines: PAL-CBL-VI) and striato-nigral connectivity (PUT-SN) (**Table 1**). There were no connections that showed significant differences between PMC-TMS compared to Sham. Overall, these findings demonstrate two important points. 10 Hz rTMS to PSC interleaved with writing task predominantly changed subcortical brain connectivity. Second, changes in brain connectivity induced by TMS may explain the differential effect of stimulation sites on behavioral outcomes.

TMS-induced activation of PSC is associated with a reduction in writing dysfluency. We next asked if there was a relationship between TMS-induced brain activation and behavior changes and if this relationship was dependent on the stimulation site. A brain activity-behavior correlational analysis was performed for all brain regions in **Table 1** that showed significant differences in functional connectivity between PSC-TMS and Sham. Among all these regions, only PSC BOLD activity showed a significant correlation with peak acceleration behavior. Specifically, TMS-induced increase in PSC BOLD activity was associated with a significant reduction of peak accelerations in WC participants ($R = -0.84$, $p = 0.02$) (**Fig. 8**). In contrast, no brain-behavior correlations were observed after TMS to PMC ($R = -0.39$, $p = 0.75$) or Sham ($R = 0.15$, $p = 0.76$). When compared across TMS conditions, there was a significant difference in brain activity-behavior association between PSC-TMS and Sham (PSC vs. Sham = -3.32, $p = 0.0084$ generalized regression and multiple comparisons corrected). Collectively, these results suggest that TMS-induced changes in the association between brain activity and behavioral measures were dependent on the stimulation site, and TMS-induced activation of PSC was associated with a reduction in writing dysfluency.

Reorganization of the motor network after PSC-TMS was associated with reduced writing dysfluency. Lastly, we explored if there was an association between TMS-induced changes in functional connectivity and behavior in the motor network and if this association was dependent on the stimulation site. From this analysis, we made three observations (**Fig. 9**). First, under Sham-TMS condition (untreated dystonia), nine significant FC relationships with writing dysfluency were identified, with the majority of them in connection to the cerebellum (cortico-cerebellum, subcortical-cerebellum, intra-cerebellum). Second, compared to the Sham, correlations between writing

dysfluency and FC involving the cerebellum were no longer present following 10 Hz rTMS at either PMC or PSC. The loss of FC-behavior correlations in these regions was observed to a greater extent after PSC-TMS than PMC-TMS. Third, PSC-TMS differed from the other stimulation sites in brain-behavior correlations at cortical (PSC-SPC) and subcortical (CAU-SN, PUT-PAL, PUT-SN) brain regions (**Fig. 9B, indicated by the "+" sign**). Of these cortical and subcortical connections, PSC-TMS significantly differed from Sham in brain-behavior associations at the cortico-cortical (PSC-SPC) connection (PSC vs. Sham: -14.6, p = 0.075, generalized regression, multiple comparisons corrected) (**Fig. 9A**). Collectively, these results demonstrated that reduced writing dysfluency after PSC-TMS may be mediated by loss of brain-behavior associations to the cerebellum, and/or gain of brain-behavior associations to cortical and subcortical brain regions. Furthermore, the association between writing dysfluency and intracortical connectivity (PSC-SPC) may be a key signature for brain-behavior changes after PSC-TMS.

Overall, TMS target comparison demonstrated that 10 Hz rTMS to the primary somatosensory cortex but not the premotor cortex significantly changed functional connectivity and markedly redistributed brain-behavior associations that spanned cortical and subcortical regions of the motor network.

DISCUSSION

The present study compared the efficacy of two TMS cortical sites in reducing dystonic behavior, each previously shown to be beneficial in separate dystonia studies, and aimed to identify the TMS-induced brain mechanism underlying the observed behavioral improvement. We report three key findings. First, 10 Hz rTMS to the primary somatosensory cortex significantly reduced writing dysfluency compared to Sham and 10 Hz rTMS to the premotor cortex. These results establish the efficacy of 10 Hz rTMS to the PSC for future clinical trials in this rare brain disorder. Second, we identified that TMS to the same region may have improved behavior by changing subcortical connectivity in the motor network. Third, we demonstrate that the intra-cortical connectivity between primary somatosensory and superior parietal cortices is a key predictor for effective stimulation at PSC. Collectively, the present study represents the first deep phenotyping of the brain and behavior changes induced by TMS in a dystonia cohort. Findings will guide future refinements in TMS protocols to achieve clinically meaningful and enduring benefits in this rare brain disorder.

Our first principal study finding was that 10 Hz rTMS to PSC significantly reduced writing dysfluency in WC dystonia. The twenty-minute PSC-TMS session showed an effect size of 0.96 compared to Sham. This effect size is among the highest reported for TMS studies in dystonia. Since the cortical gyri for PSC and PMC lie adjacent to the central sulcus, the differential stimulation response to these regions also demonstrated the cortical selectivity of our TMS effect. It is interesting that prior (9/18) studies reported a behavioral benefit after PMC-TMS (3). The majority of these studies, however, delivered 1 Hz rTMS to PMC. Therefore, the finding that PSC is a more effective stimulation site than PMC may vary by stimulation frequency. Specifically, this study showed that PSC may be more effective than PMC using 10 Hz rTMS frequency. Future

studies are needed to test if PMC or PSC may be more effective using 1 Hz rTMS frequency. Additionally, the brain state during TMS delivery may also affect the stimulation site efficacy. In this study, TMS was interleaved with a writing task to ensure the motor circuit was engaged during brain stimulation, while in prior studies, TMS was interleaved with periods of rest. Since the brain state during stimulation delivery can change the plasticity-inducing mechanism (long-term potentiation vs. long-term depression) (24), the stimulation at rest in prior studies may have induced a plasticity mechanism that may be different than the present study. Overall, our study expands the range of effective TMS parameters for adult focal hand dystonia and raises the possibility that the efficacy of the stimulation site may be a function of the stimulation frequency and brain state during TMS delivery.

Our second principal finding was that 10 Hz rTMS to PSC induced significant changes in subcortical connectivity in the motor network. This was an important study question to guide future refinements in therapeutic applications of TMS in dystonia, where subcortical regions such as basal ganglia and cerebellum play key roles. It is unknown whether active TMS improves behavior by weakening or strengthening brain connections. Our study shows that both weakening and strengthening of connections are present resulting in TMS-induced reorganization of the motor network. The strong inverse association between stimulation site (PSC BOLD activity) and writing dysfluency behavior (Fig. 8) further supports the mechanism that TMS to PSC begins a cascade of connectivity changes, similar to a molecular signaling cascade, that collectively at the network level result in reduction of writing dysfluency behavior. Overall, the present study adds important insights to the TMS-induced brain mechanism that contributes to motor behavior benefits in dystonia.

A third novel study finding was that the behavioral benefit after PSC-TMS was specifically associated with strengthening intra-cortical connectivity between the somatosensory cortex and superior parietal cortex. This is consistent with a prior TMS study, which showed that 1 Hz rTMS to the primary somatosensory cortex also activated the superior parietal cortex in WC dystonia (25). The superior parietal cortex is critically important for somatosensory discrimination by providing a mental model of the extremity function (26). Strengthening of the somatosensory to parietal connectivity may, therefore, be a key mechanism for developing a more accurate mental model of the hand-arm function, which in turn may mediate the reduction in dysfluent writing behavior. Impairment of superior parietal cortex activation has also been reported in other adult focal dystonias, including spasmodic dysphonia and cervical dystonia (27, 28). Future studies should also compare the efficacy of TMS at the parietal cortex, premotor cortex, and somatosensory cortex to determine if the activation of the parietal cortex may be a more effective target for improving somatosensory dysfunction in focal dystonias.

To our knowledge, this is the first interventional study to identify relationships between brain connectivity and dystonic behavior in the untreated dystonia syndrome to inform the pathophysiology. A prior study using a systematic review of lesion-induced dystonia across 359 published cases identified that focal upper limb dystonia was most commonly caused by lesions in the basal ganglia and thalamus (29). The present study

also supports these findings by demonstrating that three of the four brain-behavior connections that differentiate the effective stimulation site of PSC from noneffective stimulation sites of PMC and Sham conditions are connections to or within the basal ganglia regions (caudate-substantia nigra, putamen-pallidum, putamen-substantia nigra). More importantly, the present study demonstrates that the brain connectivity pattern of subregions of the motor network is responsive to change in a direction that improves behavior after PSC-TMS compared to Sham. This brain connectivity to behavior patterns can, therefore, be used as a screening tool for future interventional trials in dystonia.

The brain-behavior relationships identified in this study also provide greater insight into the cerebellum's role in dystonia. Prior neuroimaging studies observed that greater disease duration in WC participants correlated with negative cortico-cerebellar connectivity (14). Our study also identified cortico-cerebellar circuitry as potentially clinically relevant. WC participants after Sham showed a direct correlation between cortico-cerebellar connectivity and writing dysfluency, a relationship that was absent after PSC-TMS. Our results further support a causal role of this circuitry because TMS to PSC leads to less writing dysfluency and a significant loss of correlation between cortico-cerebellar connectivity and writing dysfluency. Our study also proposes key associations between subcortical-cerebellum and intra-cerebellar connectivity and behavior of writing dysfluency that warrant further investigation in future studies.

A key role of the cerebellum has also been described in individuals with cervical dystonia. A brain network derived from lesion network mapping and applied in rest-fMRI from cervical dystonia and healthy controls demonstrated that positive connectivity to the cerebellum and negative connectivity to the somatosensory cortex were specific markers for cervical dystonia (30). Furthermore, two weeks of cTBS-TMS to the bilateral cerebellum resulted in clinical improvement in cervical dystonia (31). In DYT1-TOR1A dystonia, tractography examining cerebellar outflow tracts showed that lower measures of white matter were associated with poorer performance in a sequence learning task (32). To the extent that other dystonias may share circuit mechanisms involving reduced cerebellar connectivity, our results advance the potential for 10 Hz rTMS to PSC to be used as a corrective approach.

There are several limitations of the present study to discuss. First, this study consisted of a small study cohort. Nonetheless, our approach here is that small, focused studies that deeply phenotype brain-behavior relationships using a within-subject repeated study design, as performed in the present study, can provide key insights into brain-behavior relationships in individuals with a disease to guide clinical care (33). Second, this study only examined acute responses. Future studies are needed to examine the longevity of this TMS effect and explore whether increasing stimulation sessions prolongs the duration of behavioral effects. Third, a potential confounding effect of the present study is that two active stimulations and one Sham condition were randomly assigned to each participant across three sequential study visits. Future studies dedicated to a single stimulation site would remove this potential confound and allow us to evaluate the longevity of each TMS condition. A fourth limitation of the present study is that we constrained analyses to the motor network because of its relevance to

dystonia and to reduce multiple hypothesis testing in a study with limited group sizes. There may be significant effects in regions outside of the motor circuitry that warrant consideration if we use larger dystonia study cohorts.

CONCLUSION

In summary, identifying the optimal stimulation site for engaging and improving the abnormal motor circuit mechanisms in dystonia is a major goal necessary for effectively applying TMS-related interventions for dystonia. This study used a within-participant, Sham-controlled study design in writer's cramp dystonia, coupled with functional neuroimaging and behavior, to address these unknowns. Demonstrating that TMS to PSC provides a significant behavioral benefit is a critical first step in moving TMS toward clinical therapy for dystonia. Furthermore, delineating the TMS-induced corrective changes in the motor network associated with behavioral improvement in dystonia generates mechanistic hypotheses to guide future therapeutic interventions. The pattern of brain-behavior changes observed after PSC-TMS in this study may also serve as a brain signature for a clinical response to use as a screening tool with other interventional modalities.

Data statement: All data and codes are available upon reasonable request.

Authorship contribution statement: NBP, MWL, HRA, LGA, SWD, AVP, and NC conceptualized the study. NBP, TKT, EW, and LB collected study data. NBP, PJM, MWL, RG, ZH, MD, ZBS, SG, ML, MF and AMM performed data analysis. PT and BS performed clinician rating scales. CP and JV provided software codes to assist with data collection and analysis. MWL and HRA critiqued the statistical analysis. MWL, SWD, AMM, AVP, and NC critiqued the data analysis. NBP and NC wrote the manuscript. All co-authors reviewed and edited the manuscript.

Conflict of interest: All authors report no conflicts of interest.

Declaration of competing interests: NBP serves as a member of the DMRF Medical and Scientific Advisory Council. AVP serves on the editorial board of the Brain Stimulation journal. AVP is an inventor of patents and patent applications on transcranial magnetic stimulation technology and has received patent royalties and consulting fees from Rogue Research; equity options, scientific advisory board membership, and consulting fees from Ampa Health; equity options and consulting fees from Magnetic Tides; consulting fees from Soterix Medical; equipment loans from MagVenture; and research funding from Motif. SWD has received consulting fees from Neuronetics. None of these sources played a role in the design, collection, analysis, interpretation of the data, or in the decision to submit the manuscript for publication. PJM, MWL, RG, ZH, MD, ZBS, SG, ML, TKT, EW, LB, CP, JTV, LGA, HRA, AMM and NC report no relevant financial disclosures.

Acknowledgements: This work was supported by grants to NBP from Dystonia Medical Research Foundation (Clinical Fellowship Training Program), Doris Duke Charitable Foundation (Fund to Retain Clinician Scientists), American Academy of

Neurology (career development award) and NIH NCATS (1KL2TR002554). NBP was also supported by a career development award from the Dystonia Coalition (NS065701, TR001456, NS116025) which is part of the National Institutes of Health (NIH) Rare Disease Clinical Research Network (RDCRN), supported by the Office of Rare Diseases Research (ORDR) at the National Center for Advancing Translational Science (NCATS), and the National Institute of Neurological Diseases and Stroke (NINDS). AVP's contributions were supported in part by the National Institutes of Health (R01MH128422, R01NS117405). The content is solely the responsibility of the authors and does not necessarily represent the official views of the funding agencies.

REFERENCES

1. Ortiz R, Scheperjans F, Mertsalmi T, Pekkonen E**.** The prevalence of adult-onset isolated dystonia in Finland 2007-2016. PLoS One. 2018;13(11):e0207729.
2. Albanese A, Bhatia K, Bressman SB, Delong MR, Fahn S, Fung VS, et al. Phenomenology and classification of dystonia: a consensus update. Mov Disord. 2013;28(7):863-73.
3. Morrison-Ham J, Clark GM, Ellis EG, Cerins A, Joutsa J, Enticott PG, et al. Effects of noninvasive brain stimulation in dystonia: a systematic review and meta-analysis. Ther Adv Neurol Disord. 2022;15:17562864221138144.
4. Strafella AP, Ko JH, Grant J, Fraraccio M, Monchi O**.** Corticostriatal functional interactions in Parkinson's disease: a rTMS/[11C]raclopride PET study. Eur J Neurosci. 2005;22(11):2946-52.
5. Hao W, Wei T, Yang W, Yang Y, Cheng T, Li X, et al. Effects of High-Frequency Repetitive Transcranial Magnetic Stimulation on Upper Limb Dystonia in Patients With Wilson's Disease: A Randomized Controlled Trial. Front Neurol. 2021;12:783365.
6. Voyvodic JT**.** Real-time fMRI paradigm control, physiology, and behavior combined with near real-time statistical analysis. Neuroimage. 1999;10(2):91-106.
7. Esteban O, Ciric R, Finc K, Blair RW, Markiewicz CJ, Moodie CA, et al. Analysis of task-based functional MRI data preprocessed with fMRIPrep. Nat Protoc. 2020;15(7):2186-202.
8. Awiszus F**.** TMS and threshold hunting. In: Elsevier, ed. In Supplements to Clinical neurophysiology; 2003:13-23.
9. Smith JE, Peterchev AV**.** Electric field measurement of two commercial active/Sham coils for transcranial magnetic stimulation. J Neural Eng. 2018;15(5):054001.
10. Dannhauer M, Huang Z, Beynel L, Wood E, Bukhari-Parlakturk N, Peterchev AV**.** TAP: targeting and analysis pipeline for optimization and verification of coil placement in transcranial magnetic stimulation. J Neural Eng. 2022;19(2).
11. Gomez LJ, Dannhauer M, Peterchev AV**.** Fast computational optimization of TMS coil placement for individualized electric field targeting. Neuroimage. 2021;228:117696.
12. Bukhari-Parlakturk N, Lutz MW, Al-Khalidi HR, Unnithan S, Wang JE, Scott B, et al. Suitability of Automated Writing Measures for Clinical Trial Outcome in Writer's Cramp. Mov Disord. 2023;38(1):123-32.
13. Vo A, Nguyen N, Fujita K, Schindlbeck KA, Rommal A, Bressman SB, et al. Disordered network structure and function in dystonia: pathological connectivity vs. adaptive responses. Cereb Cortex. 2023;33(11):6943-58.

14. Dresel C, Li Y, Wilzeck V, Castrop F, Zimmer C, Haslinger B**.** Multiple changes of functional connectivity between sensorimotor areas in focal hand dystonia. J Neurol Neurosurg Psychiatry. 2014;85(11):1245-52.
15. Gallea C, Horovitz SG, Najee-Ullah M, Hallett M**.** Impairment of a parieto-premotor network specialized for handwriting in writer's cramp. Hum Brain Mapp. 2016;37(12):4363-75.
16. Simonyan K, Cho H, Hamzehei Sichani A, Rubien-Thomas E, Hallett M**.** The direct basal ganglia pathway is hyperfunctional in focal dystonia. Brain. 2017;140(12):3179-90.
17. Zhuang P, Li Y, Hallett M**.** Neuronal activity in the basal ganglia and thalamus in patients with dystonia. Clin Neurophysiol. 2004;115(11):2542-57.
18. Argyelan M, Carbon M, Niethammer M, Ulug AM, Voss HU, Bressman SB, et al. Cerebellothalamocortical connectivity regulates penetrance in dystonia. J Neurosci. 2009;29(31):9740-7.
19. Iacono D, Geraci-Erck M, Peng H, Rabin ML, Kurlan R**.** Reduced Number of Pigmented Neurons in the Substantia Nigra of Dystonia Patients? Findings from Extensive Neuropathologic, Immunohistochemistry, and Quantitative Analyses. Tremor Other Hyperkinet Mov (N Y). 2015;5.
20. Kaji R, Bhatia K, Graybiel AM**.** Pathogenesis of dystonia: is it of cerebellar or basal ganglia origin? J Neurol Neurosurg Psychiatry. 2018;89(5):488-92.
21. Gianni C, Pasqua G, Ferrazzano G, Tommasin S, De Bartolo MI, Petsas N, et al. Focal Dystonia: Functional Connectivity Changes in Cerebellar-Basal Ganglia-Cortical Circuit and Preserved Global Functional Architecture. Neurology. 2022;98(14):e1499-e509.
22. Dadi K, Varoquaux G, Machlouzarides-Shalit A, Gorgolewski KJ, Wassermann D, Thirion B, et al. Fine-grain atlases of functional modes for fMRI analysis. Neuroimage. 2020;221:117126.
23. Horovitz SG, Gallea C, Najee-Ullah M, Hallett M**.** Functional anatomy of writing with the dominant hand. PLoS One. 2013;8(7):e67931.
24. Enomoto H, Terao Y, Kadowaki S, Nakamura K, Moriya A, Nakatani-Enomoto S, et al. Effects of L-Dopa and pramipexole on plasticity induced by QPS in human motor cortex. J Neural Transm (Vienna). 2015;122(9):1253-61.
25. Havrankova P, Jech R, Walker ND, Operto G, Tauchmanova J, Vymazal J, et al. Repetitive TMS of the somatosensory cortex improves writer's cramp and enhances cortical activity. Neuro Endocrinol Lett. 2010;31(1):73-86.
26. Kaas J**.** Somatosensory System. In: JK PGM, ed. The Human Nervous System. London: Elsevier Academic Press; 2004:1061-93.
27. Battistella G, Simonyan K**.** Top-down alteration of functional connectivity within the sensorimotor network in focal dystonia. Neurology. 2019;92(16):e1843-e51.
28. Naumann M, Magyar-Lehmann S, Reiners K, Erbguth F, Leenders KL**.** Sensory tricks in cervical dystonia: perceptual dysbalance of parietal cortex modulates frontal motor programming. Ann Neurol. 2000;47(3):322-8.
29. Corp DT, Greenwood CJ, Morrison-Ham J, Pullinen J, McDowall GM, Younger EFP, et al. Clinical and Structural Findings in Patients With Lesion-Induced Dystonia: Descriptive and Quantitative Analysis of Published Cases. Neurology. 2022;99(18):e1957-e67.

30. Corp DT, Joutsa J, Darby RR, Delnooz CCS, van de Warrenburg BPC, Cooke D, et al. Network localization of cervical dystonia based on causal brain lesions. Brain. 2019;142(6):1660-74.
31. Koch G, Porcacchia P, Ponzo V, Carrillo F, Caceres-Redondo MT, Brusa L, et al. Effects of two weeks of cerebellar theta burst stimulation in cervical dystonia patients. Brain Stimul. 2014;7(4):564-72.
32. Carbon M, Argyelan M, Ghilardi MF, Mattis P, Dhawan V, Bressman S, et al. Impaired sequence learning in dystonia mutation carriers: a genotypic effect. Brain. 2011;134(Pt 5):1416-27.
33. Gratton C, Nelson SM, Gordon EM**.** Brain-behavior correlations: Two paths toward reliability. Neuron. 2022;110(9):1446-9.

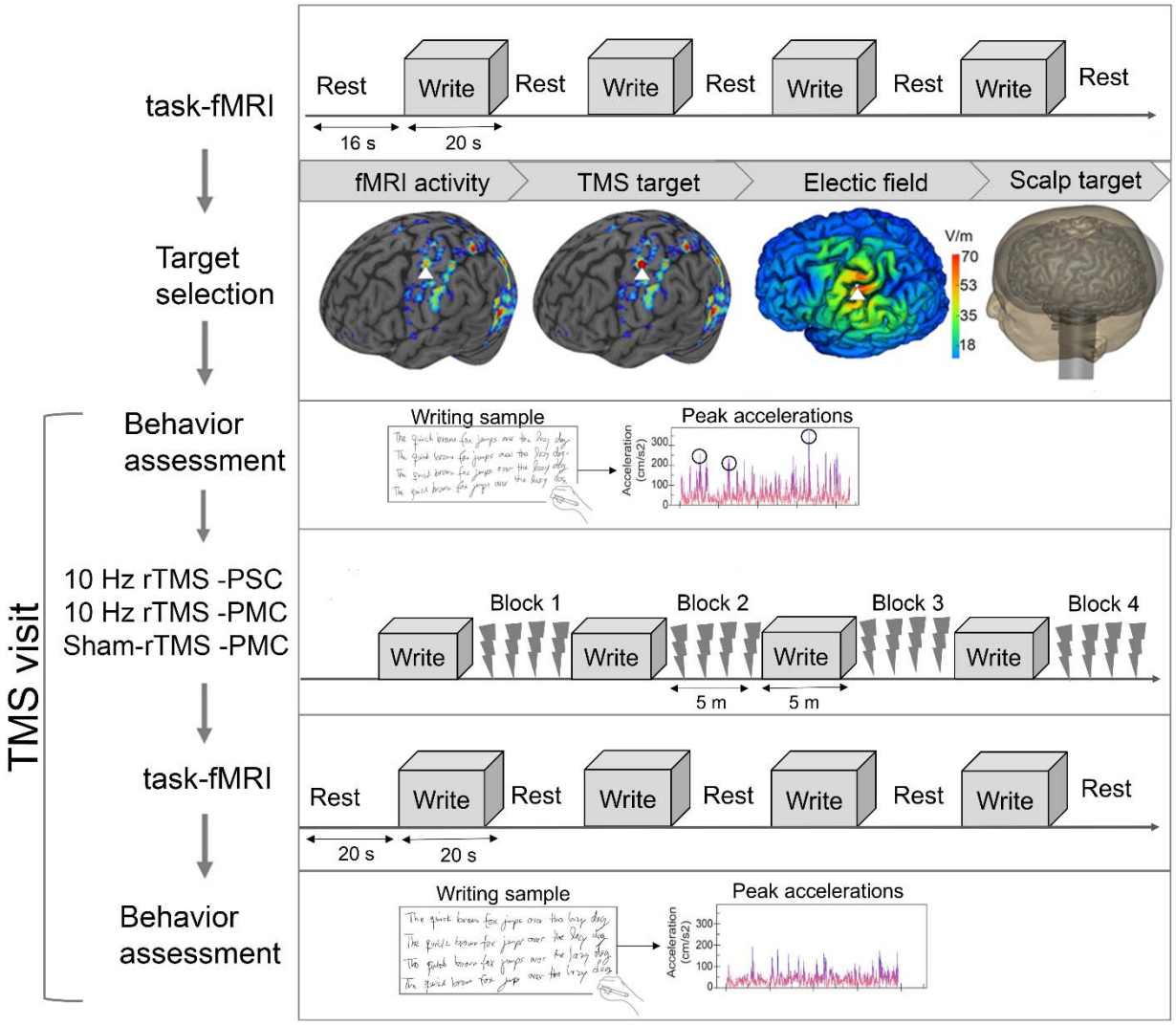

Figure 1: TMS target selection and TMS delivery. To select a scalp target for TMS delivery, each subject completed a task-based fMRI at baseline. An individualized scalp target to the motor/premotor cortex (PMC) and primary somatosensory cortex (PSC) was then prepared using fMRI and electric field modeling. Subjects received three TMS conditions: 10 Hz rTMS to PSC, 10 Hz rTMS to PMC, and Sham rTMS to PMC (total 4,000 pulses). Each TMS condition was delivered over four stimulation blocks during a single visit. To synchronize the brain state and activate the motor network during TMS delivery, stimulation blocks were interleaved with writing blocks. TMS effect was measured using writing behavior and task-based fMRI.

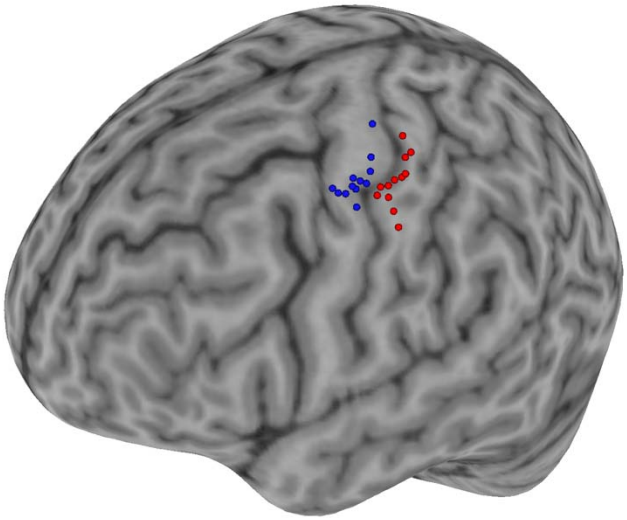

Figure 2: Individualized targets for rTMS to PMC and PSC in WC. The cortical target for rTMS delivery to the left PMC (blue) and left PSC (red) was developed using fMRI and electric field modeling. The final target for PMC-TMS and PSC-TMS for each WC participant is shown overlayed on a standard MNI brain.

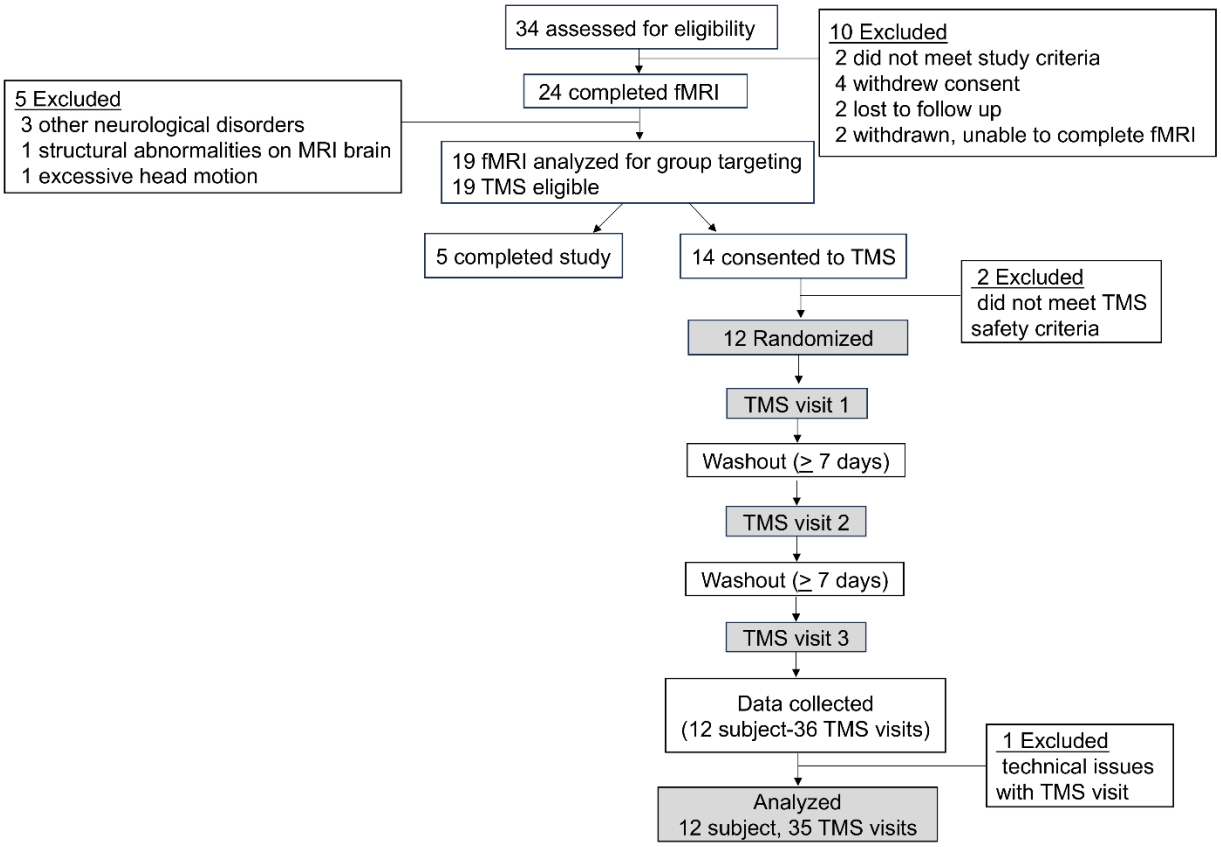

Figure 3: Consort diagram showing the recruitment, inclusion, and exclusion numbers for participants. A total of 34 WC dystonia participants were screened. Twenty-four participants completed fMRI, and 14 consented to the TMS study. Of these, 12 participants were randomized and completed the TMS study.

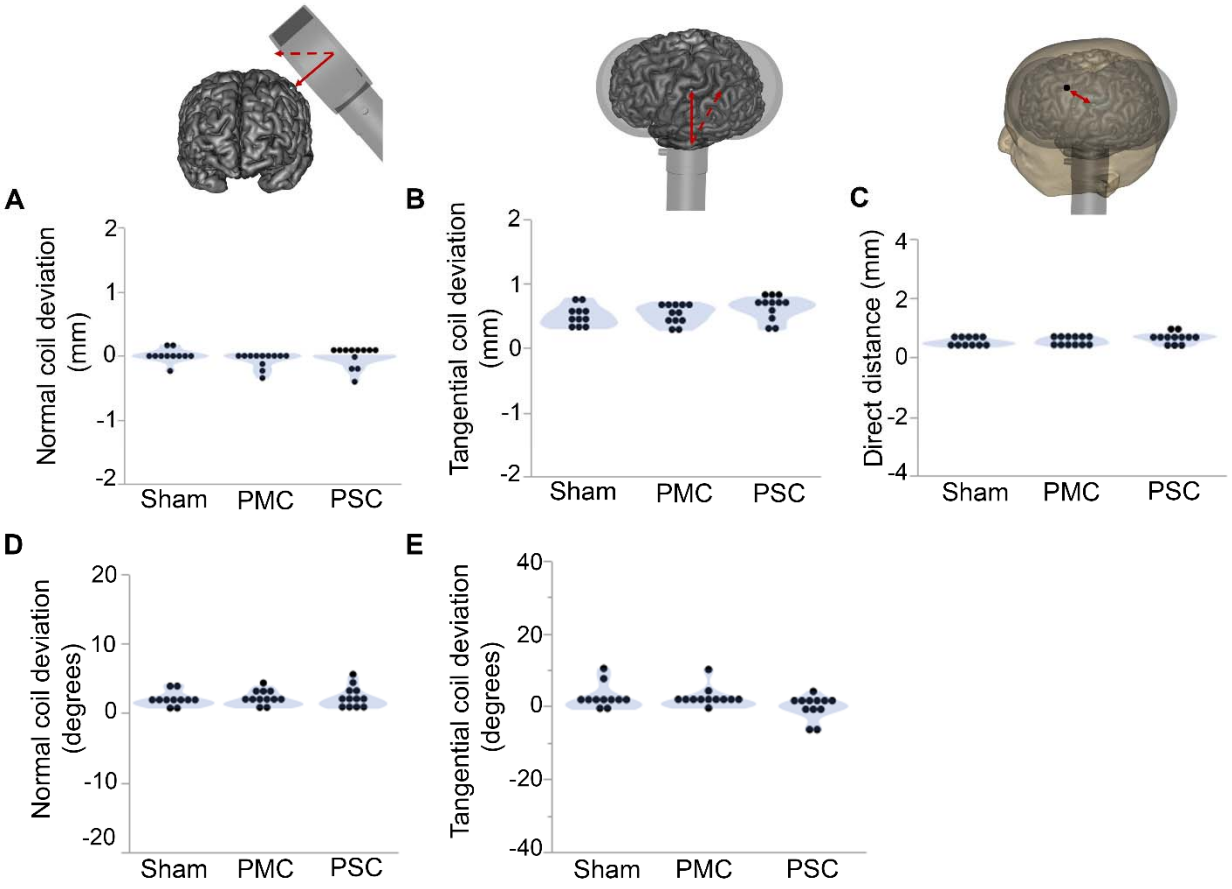

Figure 4: Minimal deviation between intended and actual TMS scalp targets. Each graph shows the deviation in the TMS coil setup, defined as the difference between the intended and actual TMS coil parameters for the three TMS conditions. The deviation in TMS coil position is measured in the normal plane (**A**) and tangential plane (**B**). The direct distance between the intended TMS coil position and the actual TMS coil position is also measured (**C**). The deviation in TMS coil orientation is also presented in the normal plane (**D**) and tangential plane (**E**). Each data point on a graph represents the mean TMS coil deviation across all four TMS blocks for each subject. Data are presented for Sham-rTMS (n = 11), 10 Hz rTMS to PMC (n = 12), and 10 Hz rTMS to PSC (n = 12).

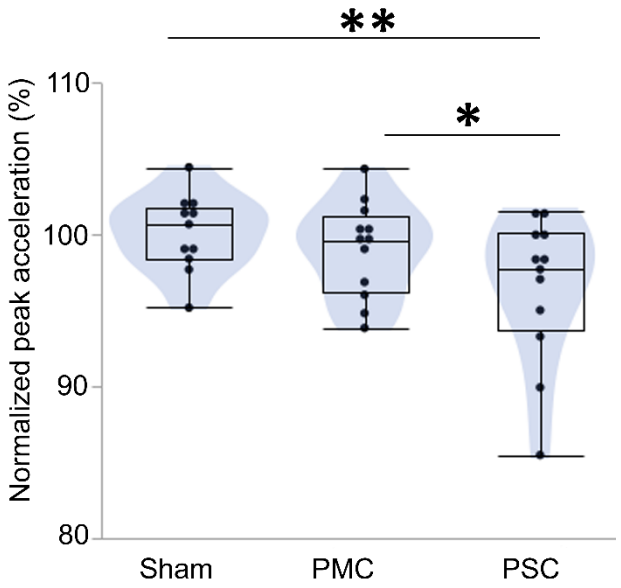

Figure 5: 10 Hz rTMS to PSC, but not PMC, reduced writing dysfluency in WC. 10 Hz rTMS to PSC significantly reduced a measure of writing dysfluency called peak accelerations compared to Sham-TMS in a within-subject analysis in WC subjects. PMC did not show significant differences in writing dysfluency compared to Sham-TMS. Each data point represents the mean change in peak accelerations for each TMS condition, with higher measures representing worsening writing dysfluency. **p<0.01, *p<0.05 after multiple comparisons correction.

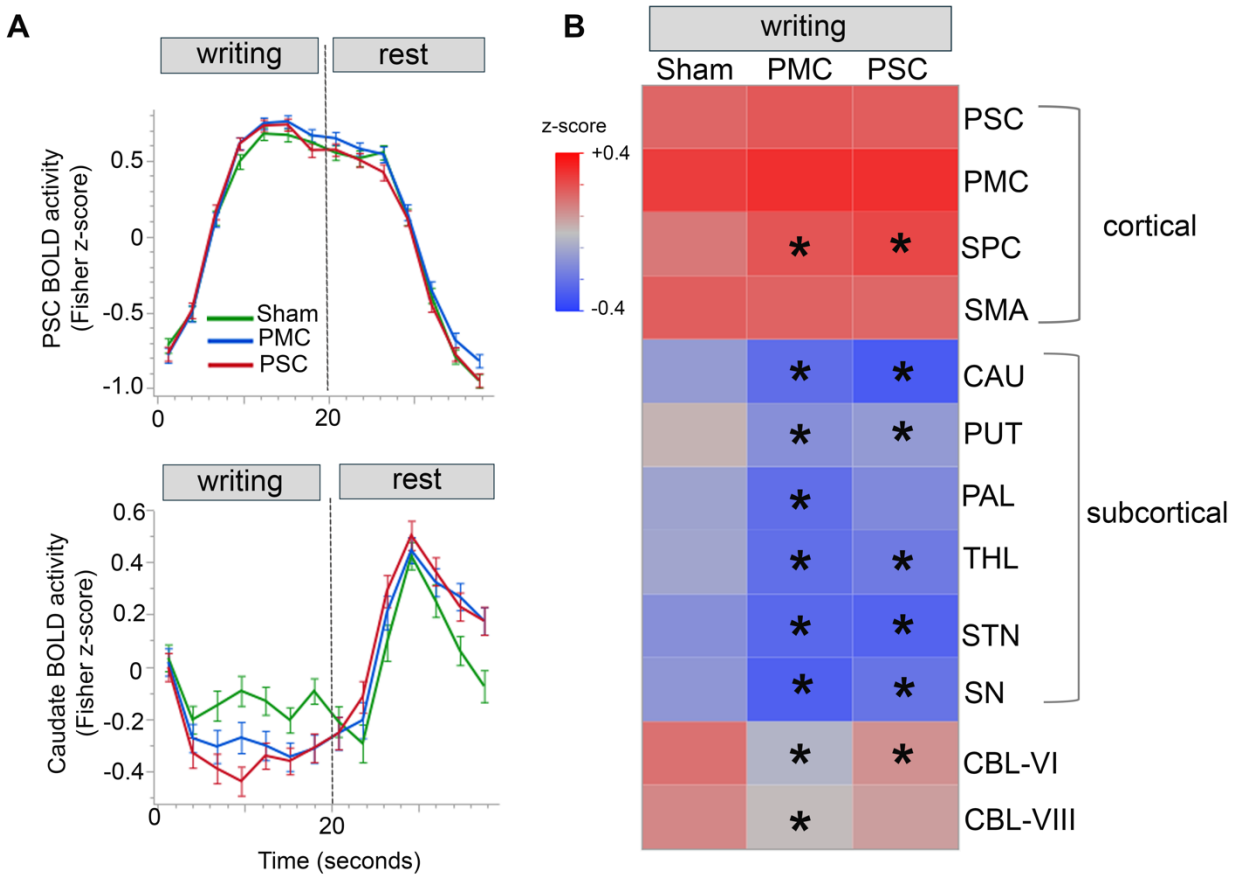

Figure 6: 10 Hz rTMS to either PMC or PSC decreased subcortical activity in the motor network. A) Graphs represent mean BOLD activity during the writing and rest blocks after each TMS condition [Sham (green), PMC-TMS (blue), and PSC-TMS (red)]. The mean BOLD activity is presented for brain regions of the primary somatosensory cortex (PSC, top graph) and caudate (bottom graph, PSC vs. Sham: -0.19, p = 1.65 x 10-5, PMC vs. Sham -0.14, p = 2.8 x 10-4, PSC vs. PMC: 0.05, p = 0.14). **B)** Heatmap represents mean BOLD activity during the writing block for subregions of the motor network across the three TMS conditions. Asterisks indicate significant differences in mean BOLD activity for PMC-TMS or PSC-TMS compared to Sham (MMRM and multiple comparisons corrected). SPC: superior parietal cortex, SMA: supplementary motor area, CAU: caudate, PUT: putamen, PAL: pallidum, THL: thalamus, STN: subthalamic nucleus, SN: substantia nigra, CBL-VI: cerebellum, lobule VI and CBL-VIII: cerebellum, lobule VIII.

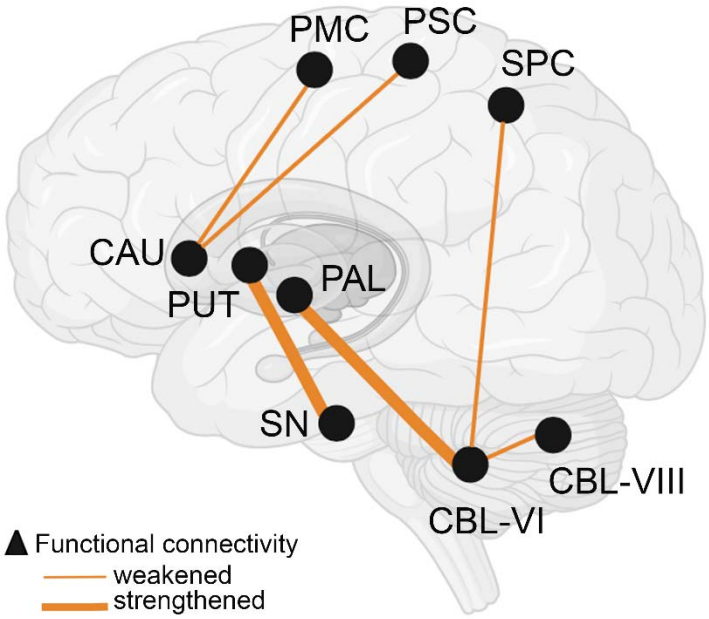

Figure 7: 10 Hz rTMS to PSC but not PMC-induced changes in cortical-subcortical connectivity in the motor network. Connectome represents TMS-induced changes in functional connectivity in the motor network. Each line represents a connection between two regions (black circles) of the motor network. Only connections that showed significant change after PSC-TMS compared to Sham were presented ($p < 0.05$ after multiple comparisons correction). There were no connections that showed significant change after PMC-TMS compared to Sham. The magnitude of connectivity change is represented by the line thickness (thin line: weakened, thick line: strengthened) and values reported in Table 1.

Table 1: Changes in functional connectivity induced by PSC-TMS compared to Sham in the motor network

Brain Regions	Functional connections	Multiple Repeated Measures Analysis			
		PSC vs. Sham Mean difference in FC (z-score)	SE (z-score)	t-ratio	p-value*
Cortico-striatal	PMC-CAU	-0.17	0.04	-4.49	0.015
	PSC-CAU	-0.13	0.03	-4.17	0.015
Cortico-cerebellar	SPC-RCBL-VIII	-0.15	0.05	-3.38	0.048
Subcortico-subcortical	PAL-CBL-VI	+0.17	0.05	3.61	0.041
	PUT-SN	+0.16	0.04	3.53	0.042
Intra-cerebellar	R-CBL VI-VIII	-0.18	0.04	-4.28	0.015
	R-CBL VI-VIII	-0.20	0.05	-4.12	0.015

SE: Standard Error, *p-values after multiple comparison adjustment

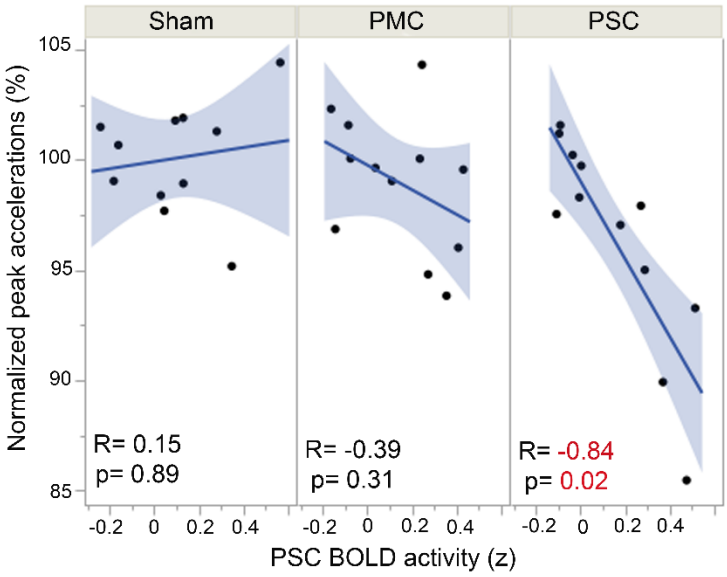

Figure 8: TMS-induced increase in BOLD activity at primary somatosensory cortex correlated with reduced writing dysfluency. Graph represents the correlation between BOLD activity at the primary somatosensory cortex (x-axis) and behavior of peak accelerations (y-axis) for the three TMS conditions. Each data point represents the correlation between a WC participant's PSC BOLD activity and peak accelerations behavior for each TMS condition. The shaded blue region represents the confidence region for the fitted lines. PSC vs. Sham difference = -3.32, p=0.0084 generalized regression and multiple comparisons corrected.

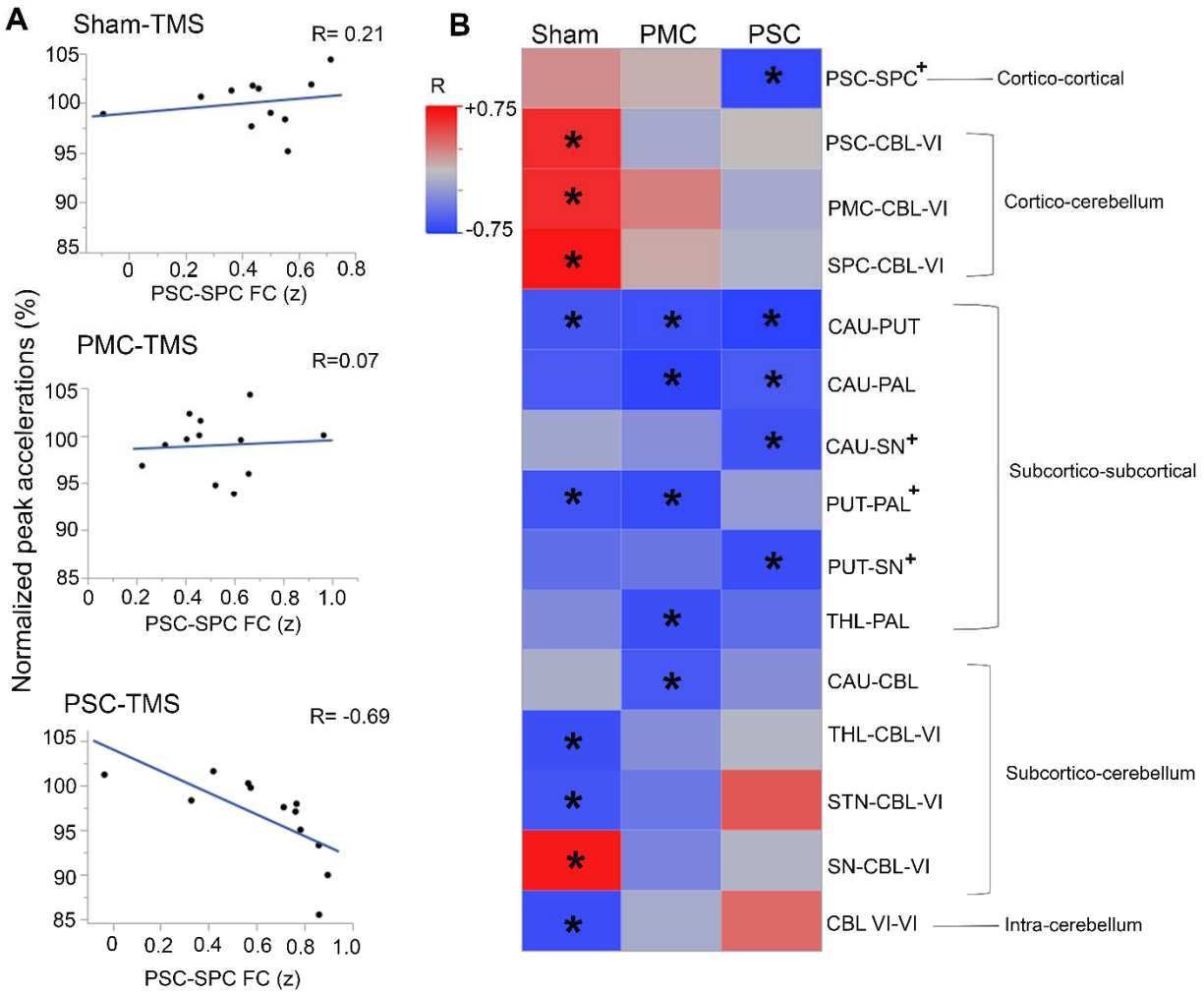

Figure 9: Reorganization of the motor network after PSC-TMS correlated with reduced writing dysfluency. A) Graph represents the correlation between functional connectivity (FC) (x-axis) and peak acceleration behavior (y-axis) for the three TMS conditions. Each data point represents a WC participant's connectivity-behavior relationship. Strengthening of connectivity between the primary somatosensory cortex and superior parietal cortex was associated with a reduction in peak accelerations behavior after PSC-TMS compared to Sham-TMS (PSC vs. Sham: -14.6, p = 0.075, generalized regression, multiple comparisons corrected). **B**) A heatmap of the brain connectivity-behavior relationship in the motor network. Each box represents the mean correlation (R) between peak accelerations behavior and a functional connection for each TMS condition. Heatmap is reported only for connections with R $\geq$ 0.6 for at least one TMS condition (indicated by an asterisk). "+" indicates connectivity-behavior relationships that are different for PSC-TMS compared to both Sham-TMS and PMC-TMS.